

Electron correlation and disorder in $\text{Hg}_{1-x}\text{Cd}_x\text{Te}$ in a magnetic field

Stuart B. Field,* D. H. Reich, and T. F. Rosenbaum

The James Franck Institute and Department of Physics, The University of Chicago, Chicago, Illinois 60637

P. B. Littlewood

AT&T Bell Laboratories, Murray Hill, New Jersey 07974

D. A. Nelson

Honeywell Electro-Optics Division, Lexington, Massachusetts 02173

(Received 6 October 1987)

We report both linear and nonlinear magnetoconductance measurements on two different density samples of similar stoichiometry $\text{Hg}_{1-x}\text{Cd}_x\text{Te}$ for $0.01 < T < 2.5$ K and $0 < H < 80$ kOe. The critical magnetic field for driving the samples through the metal-insulator transition is proportional to temperature at low T and saturates at $T \sim 2$ K, in quantitative agreement with a theory for the melting of a Wigner crystal in magnetic field. In the insulating state, we observe a non-Ohmic I - V characteristic at threshold electric fields less than 1 mV/cm. By analogy to theories for charge-density-wave depinning, we estimate that the electrons are correlated over regions of a few hundred lattice spacings. Finally, we map out the phase boundary between the low- T -high- H electron solid and the high- T -low- H correlated fluid, explicitly demonstrating the necessity of millikelvin temperatures for studying the relative roles of disorder and Coulomb interactions in the electron solid.

I. INTRODUCTION

Systems of interacting electrons exhibit a wide range of cooperative behavior at low temperature, from superconductivity to the quantum Hall effect. The theory for one such correlated electron system was formulated by Wigner¹ in 1934. He showed that at sufficiently low electron density the Coulomb interactions dominate the quantum-mechanical kinetic energy and force the electrons into a crystalline array. Experimental manifestations of the true quantum Wigner crystal are difficult to find, but advances in semiconductor and low-temperature technology over the last decade have renewed interest in this search, and theoretical models have emerged with testable predictions.

Wigner considered a collection of electrons embedded in a uniform jellium of positive charge at temperature $T=0$. The experiments which attempt to probe the Wigner-crystal state in low-electron-density, narrow-gap semiconductors differ from the theoretical ideal on at least three counts: (i) the presence of disorder in the background charge, which is inimical to the development of electron correlation, (ii) the effect of nonzero temperatures, and (iii) the need for a magnetic field to help nucleate the electron crystal. The experimental situation is further complicated by the difficulty of making structural measurements on only 10^{14} electrons/cm³ in a background lattice of 10^{23} atoms/cm³. Hence, the studies to date primarily consist of transport measurements which couple directly to the electrons.

The data have been related to either the theoretical ideal of a perfect Wigner crystal, where only correlation effects are important *or* to magnetic freeze-out, a noninteracting single-electron model where electrons bind to

individual impurities. Yet, the energies involved in both the electron-electron and electron-impurity interaction are of the same magnitude, and one legitimately cannot disregard either. A natural way to include the effects of both interactions and disorder is to describe the degree of crystalline order with a finite correlation length. The perfect electron crystal has a correlation length only limited by the size of the sample; magnetic freeze-out corresponds to a correlation length of less than one electron lattice spacing. The more likely physical situation is a correlation length somewhere in between as the electrons adjust themselves to the competition between impurity binding and Coulomb repulsion. In this paper, we report both Ohmic transport and nonlinear I - V measurements on different density samples of $\text{Hg}_{1-x}\text{Cd}_x\text{Te}$ in magnetic field which provide evidence for the collective nature of the insulating state and allow the determination of a correlation length through a scaling theory. Furthermore, we investigate explicitly the effects of finite temperature on the electron solid and map out a phase diagram. We show that the solid melts above $T \sim 1.5$ K, demonstrating the necessity of millikelvin temperatures to study the correlated electron (poly)crystal.

II. THEORY

Consider an electron gas immersed in a uniform positive neutralizing background (jellium). If the density of the electron gas is n , then the kinetic energy per electron is proportional to $n^{2/3}$ or $1/r^2$, where r is the average electron separation. The potential energy is just given by the Coulomb repulsion, proportional to $1/r$ or $n^{1/3}$. Hence, unlike the classical case, the transition into the Wigner crystal¹ occurs at low n or large r . The electrons

find it energetically favorable to get as far from each other as possible, and they do not have enough kinetic energy to move off the lattice.

Two electron systems which are possible candidates for Wigner crystallization are elemental metals and doped semiconductors. If the conduction-band electrons would localize in the metal, and if we ignore screening, then the potential energy $E_p \approx e^2/r$. Furthermore, if we approximate the effective mass m^* as the mass of the electron m , then the kinetic energy would be determined by the uncertainty principle, $E_k \approx \hbar^2/2m(r/a)^2$, where a is a parameter setting the distance by which an electron may wander from its lattice site. The Lindemann melting criterion² requires $a \leq 10$, and the crystallization condition, $E_p \gg E_k$, gives $n_W \ll 5 \times 10^{19} \text{ cm}^{-3}$. However, the elemental metal with the lowest electron density is cesium, where $n = 9.1 \times 10^{21} \text{ cm}^{-3} \gg n_W$.

Much lower electron densities can be obtained in doped semiconductors. Following the arguments above, $E_p \approx e^2/\epsilon r$, where ϵ is the dielectric constant of the crystal lattice, and $E_k \approx \hbar^2/2m^*(r/10)^2$. These expressions yield the inequality $n_W \ll (5 \times 10^{19} \text{ cm}^{-3})/[\epsilon(m/m^*)]^3$. In silicon, for example, $\epsilon(m/m^*) = 32$, giving the criterion that the dopant density $n_W \ll 2 \times 10^{15} \text{ cm}^{-3}$. Although silicon can be doped at this level, the few donor electrons simply will be pinned to impurity sites at low T .

If the disorder in the positive background charge is to be averaged over, and if the energy scale for Coulomb interactions of electrons with charged impurities is to be comparable to the Coulomb interaction between electrons, then the semiconductor must be degenerately doped. Mott's criterion for the critical density at the metal-insulator transition³ is $n_c^{1/3} a_B^* = 0.26$, where $a_B^* = \epsilon(m/m^*)a_0$ is the electron's effective Bohr radius and $a_0 = 0.53 \text{ \AA}$. This leads to the requirement that $n_c > (1 \times 10^{23} \text{ cm}^{-3})/[\epsilon(m/m^*)]^3$, whereas the requirement for Wigner crystallization was that $n_W \ll (5 \times 10^{19} \text{ cm}^{-3})/[\epsilon(m/m^*)]^3$. Clearly, these two inequalities cannot be satisfied simultaneously.

A resolution to this problem came from Durkan *et al.*,⁴ who made the suggestion that certain magnetoresistance anomalies in InSb might be due to the formation of a Wigner crystal by the donor electrons at high magnetic field. Classically, the effect of a magnetic field, H , on a charged particle is to force it into a circular orbit, with radius $l = (\hbar c/eH)^{1/2}$. Thus, in a large magnetic field along \hat{z} , we expect the electron states to be tight orbits in the x - y plane, with dispersion in the z direction. The field also serves to reduce the Fermi energy because of the formation of sharply spiked Landau levels in the density of states. At a sufficiently high magnetic field, all the electrons condense into the lowest (spin-split) Landau level and the kinetic energy is set by the magnetic length l , decreasing with field as $1/H^{1/2}$. Narrow-gap semiconductors like InSb and $\text{Hg}_{1-x}\text{Cd}_x\text{Te}$ are particularly well suited to the study of the localizing effects of magnetic fields; their light conduction-band effective masses give magnetic g factors and, hence, effective fields 2 orders of magnitude larger than the bare electron value. Furthermore, the combination of small m^* and large ϵ can give

an effective Bohr radius as large as 1000 \AA and metallic behavior for carrier densities as low as 10^{14} cm^{-3} .

The picture of long, parallel "rods" of electrons shows how they might crystallize in the x - y plane. The question of how they localize in the z direction was addressed by Kleppmann and Elliott.⁵ They used a variational technique to show that the energy of these rod states is lowered if the electrons order along the length of the rods, an ordering again brought about by the Coulomb repulsion. They found that the electrons lie in cigar-shaped wave packets, elongated in the direction of the field. Thus, they predicted a three-dimensional, but anisotropic Wigner crystal. Kleppmann and Elliott also estimated the melting temperature of the crystal, based on calculations of the crystal's cohesive energy and using the Lindemann criterion. Following their approach, one may construct a phase diagram in the H - T plane.

The problem of the Wigner crystal in magnetic field was treated as well by Gerhardt,⁶ who used the Hartree-Fock approximation to construct a phase diagram without resorting to the Lindemann criterion. However, Gerhardt finds the unphysical result that at large H the melting temperature should decrease with increasing H . This is no doubt an artifact of the Hartree-Fock approximation, which gives a continuous melting transition. Physically, we expect the melting temperature to saturate^{1,5} in the large-field limit.

None of these theoretical treatments address the important question of disorder. In a doped semiconductor, in particular, we know that disorder will be important because of the presence of charged donor impurities. Disorder is antagonistic to the formation of a Wigner-crystal phase; in three dimensions, one expects that there will be no true long-range order even if the disordering potential is weak. Nevertheless, if the effects of disorder are small the crystalline order should persist up to some correlation length L , which may be much larger than the Wigner-crystal lattice spacing $R_0 = n^{-1/3}$. With increasing disorder the correlation length shrinks; once $L \sim R_0$ the state is better described as an "electron glass."⁷

Even when L is large, random impurities and other disorder will pin the electron lattice. This pinning leads to two experimentally observable effects. First, we expect a degenerately doped semiconductor to undergo a metal-insulator transition as the magnetic field is increased. The electrons condense into a pinned electron state and the conductivity drops precipitously. Any remnant conductivity is probably a finite-temperature effect due to thermally excited electrons or, possibly, to diffusion along the electron-crystal grain boundaries.⁸ Second, it should be possible to depin the crystal by application of an electric field. This depinning will manifest itself as an increase in conductivity at some threshold field E_d , that is, as a nonlinear I - V characteristic.

We estimate the depinning field by using the analysis previously applied to sliding charge-density waves.⁹ The correlation length L is determined by a competition between the elastic stiffness of the electron lattice and the local random potential. A classical model Hamiltonian describes the interaction of the electron lattice with the underlying potential Φ , valid for $L \gg R_0$:

$$H = \int d^3r \left[\frac{1}{2} K |\nabla u|^2 + \rho_c E u + \sum_i \Phi_i(r - u(r) - R_i) \right].$$

Here $u(r)$ is the local distortion of the electron lattice, $K \sim e^2 R_0^{-4} \epsilon_\infty^{-1}$ the shear modulus of the lattice, and Φ_i the potential due to impurities at positions R_i or other disorder. If L is large compared to the average impurity spacing $c^{-1/3}$, where c is the impurity concentration, then L is determined by the expression

$$K(R_0/L)^2 \approx (c \langle \Phi^2 \rangle / L^3)^{1/2},$$

where $\langle \rangle$ denotes a spatial average. The electric field E couples to the full charge density $\rho_c \approx ne$; thus, the threshold for sliding will be approximately

$$E_d \approx A(K/\rho_c R_0)(L/R_0)^{-2},$$

where A is a numerical prefactor of order unity. This estimate does not require any assumptions about the strength of the potential Φ ; however, if the impurity potential were to dominate, then $L/R_0 \approx 1$ and the above analysis would not apply. In this strong-pinning limit, the electrons are strongly correlated with individual impurities, and hardly at all with each other. This situation is usually called magnetic freeze-out.

In summary, the theoretical picture of a Wigner crystal in a doped semiconductor looks as follows. At low magnetic fields H , the sample is metallic. As H is increased, the electrons suddenly coalesce into a crystalline phase, with a concomitant drop in conductivity. The crystal may be melted by increasing the temperature sufficiently. In a low electric field, the domains of the electron crystal are pinned to impurities. An increase in the electric field beyond E_d depins the crystal, leading to nonlinear I - V characteristics. The correlation length L can be estimated from the value of E_d .

Other instabilities are also possible if the band structure is not simple. If the spin splitting between bands is small so that both spins are occupied in the extreme quantum limit, then a spin-density wave may form. This is a possibility in the case of graphite at very large (≈ 200 kOe) magnetic fields.¹⁰ In a multivalley semiconductor, an instability toward the formation of "valley density waves" may occur.¹¹ Neither of these situations is realized in the case of $\text{Hg}_{1-x}\text{Cd}_x\text{Te}$, which has a single conduction band and a spin splitting of roughly half the cyclotron energy.

III. EXPERIMENTAL BACKGROUND

We confine ourselves here to discussions of the work on narrow-gap semiconductors, but note the extensive literature on related systems such as colloidal crystals,¹²

graphite in high magnetic field,¹⁰ heavy-ion plasmas,¹³ and electrons on the surface of helium.¹⁴ Narrow-gap semiconductors are attractive candidates for studying Wigner crystallization because they can satisfy the Mott criterion for metallic behavior at donor density as low as 10^{14} cm^{-3} , while the small effective masses of the carriers allows the extreme quantum limit, and, subsequently, the insulating state to be reached at magnetic fields of only a few kilo-oersteds. The alloy $\text{Hg}_{1-x}\text{Cd}_x\text{Te}$ is especially appealing because many parameters of the system¹⁵ (e.g., band gap and effective mass) may be varied continuously by changing the Cd concentration x . Pure CdTe is a semiconductor with a band gap of 1.58 eV. Pure HgTe is a semimetal where the conduction and valence bands overlap by 0.28 eV. The solid solution, $\text{Hg}_{1-x}\text{Cd}_x\text{Te}$, has a semimetal-semiconductor transition at $x=0.146$. As x is reduced from 1, the conduction and valence bands approach each other, the curvature of the conduction band increases, and m^* decreases rapidly. When the bands touch, the curvature is infinite and $m^*=0$.

The semiconducting wafers used in our experiments were oriented single crystals grown at Honeywell by a new process referred to as the DME technique.¹⁶ This seeded bulk-growth method enables significant improvements over conventional growth techniques in the areas of crystallinity, purity, compositional uniformity, precipitate density, and reproducibility. The total variation in x across a 15-mm-diam wafer is in general less than 0.008; in the particular samples we used, it was always less than 0.003. The $T=77$ K mobilities of these crystals are also typically 50% higher than those grown by conventional methods. The samples are doped to the required donor density with Ga or In impurities. We studied intensively samples cut from two wafers, referred to in the text as S1 and S2. The relevant parameters of these two wafers are given in Table I.

A. Sample preparation

Three technical problems had to be overcome in order to make reliable samples from the high-quality Honeywell wafers. The first of these was an oxide surface layer that developed over time, which could lead to anomalous results. The second was a sensitivity to high ($> 100^\circ\text{C}$) temperatures which could change the sample's carrier density. The final problem was $\text{Hg}_{1-x}\text{Cd}_x\text{Te}$'s extreme brittleness, which demanded that delicacy be exercised in handling the material.

Questions about the existence and effects of a surface oxide layer on $\text{Hg}_{1-x}\text{Cd}_x\text{Te}$ have concerned many workers.¹⁷⁻²¹ There now seems to be no doubt that such a layer may in fact be grown, and that it greatly affects the

TABLE I. Parameters of the $\text{Hg}_{1-x}\text{Cd}_x\text{Te}$ samples used in the experiments.

Sample	x	n (10^{14} cm^{-3})	m/m^*	ϵ_∞	μ ($T=77$ K) ($\text{cm}^2/\text{V sec}$)
S1	0.2378	1.40	80	20	150 000
S2	0.2250	2.30	95	20	171 000

low-temperature properties. Mullin and Royle¹⁷ present data which show how a purposely induced layer introduces changes of sign in the low-temperature Hall coefficient of $\text{Hg}_{1-x}\text{Cd}_x\text{Te}$, and also show how proper surface treatment—in their case, etching the surface in a bromine bath—may be used to eliminate such anomalous behavior.

The electrical properties of $\text{Hg}_{1-x}\text{Cd}_x\text{Te}$ can be influenced by high temperatures as well. It is believed that *p*-type conductivity in $\text{Hg}_{1-x}\text{Cd}_x\text{Te}$ is due to acceptor levels caused by Hg vacancies. At high temperature, the volatile Hg may actually evaporate from the surface, leaving vacancies which eventually diffuse throughout the sample.²² This effect may be large enough to change a crystal's doping from *n* to *p* type.

Finally, there is the problem of the crystal's extreme mechanical brittleness. The wafers are very difficult to cut without introducing small stress fractures invisible to the eye, which later cause the sample to break under the stresses of cooling to millikelvin temperatures. Any cutting or contacting method must be gentle enough not to introduce these small cracks.

In light of these concerns, samples were prepared in the following manner.

(i) The $\text{Hg}_{1-x}\text{Cd}_x\text{Te}$ wafers were waxed to a holder and cut to shape (typically bars $2 \times 0.5 \times 10 \text{ mm}^3$) on a South Bay Technology low-speed diamond saw. The cutting speed was limited to $\sim 10 \text{ in./s}$, and the wafer was waxed between a microscope slide and a cover slip, with pieces of glass slide surrounding the sample to provide support. The temperature of the wax was never allowed to exceed 100°C as measured by a thermocouple embedded in the wax.

(ii) The wax was removed with paint thinner. Mechanical wiping of the sample, while effective, too often caused cracking. Instead, the samples were dipped into three successive baths of hot (but again under 100°C) paint thinner for 10 min each, followed by a rinse in room-temperature methanol.

(iii) Correctly etching the samples was a particularly important step. The etch serves to remove the oxide layer which not only may obscure the physics, but makes it very difficult to attach good solder contacts. The sample was placed (using a polypropylene holder) in a bath of 10% (by volume) Br in methanol for 30–60 s, followed by a second bath in a 1% solution for the same length of time. It was then rinsed two or three times in pure methanol and, finally, in purified water. In all of these procedures, the cleanliness of the containers and the purity of the etchants is important. This method leaves a bright, clean surface receptive to soldering.

(iv) Pure indium solder contacts were attached to the surface or edge of the sample using a suitably modified Fibrasonics ultrasonic soldering iron. The tip of the iron was turned down to a small point and replated with iron, and a Variac was installed in its power supply to lower the tip temperature to the melting point of indium. The sample was supported by suction to reduce strain and the soldering was done under a $\sim 40\times$ stereo microscope. Finally, 0.002-in. $\text{Au}_{0.98}\text{Sn}_{0.02}$ wires were attached to the desired number of indium contacts in place.

B. Method

Within minutes of preparation, samples were top loaded into an Oxford Instruments Model 200 helium dilution refrigerator and subsequently cooled to $T = 10 \text{ mK}$. The ability to top load quickly into a cold high vacuum helped prevent the buildup of any oxide layer. Longitudinal and Hall resistivities were measured both by conventional five-probe and van der Pauw²³ methods, with the use of a lock-in technique at 16 Hz. The results were frequency independent up to a few hundred Hz. Samples could be mounted parallel to or perpendicular to the field of a 100-kOe superconducting solenoid which was typically ramped at 0.006 kOe/s at low T . Nonlinear I - V curves were obtained using both ac and dc methods. In the former, the sample current simply is supplied by the reference output of the Princeton Applied Research (PAR) 124A lock-in amplifier and deviations from linearity mark the effect. Unfortunately, the ac field averages over the depinning voltage, smearing the sharp threshold. The dc method corrects this problem by using a dc current through the sample with a small superimposed ac ripple (typically 5% of the maximum dc current). The PAR 124A with a 116 preamplifier then measures the differential resistance, dI/dV , directly.

IV. RESULTS

Historically, magnetotransport measurements on the narrow-gap semiconductors $\text{Hg}_{1-x}\text{Cd}_x\text{Te}$ and InSb have been a source of controversy. They have been variously interpreted as evidence for a magnetic-field-induced Mott transition,²⁴ electron localization into a Wigner lattice^{25,26} or viscous electron fluid,²⁷ or magnetic freeze-out of the free carriers.^{28–31} We believe that our results allow a more definitive probe of the relative roles of electron correlation and disorder because of (i) higher-quality samples, (ii) a temperature range from millikelvin, well below the characteristic energies in the problem, to a few kelvin, comparable to both the electron-electron and electron-impurity interaction energies, and (iii) the observation of a nonlinear conduction process at electric fields of less than 1 mV/cm , analogous to phenomena studied in charge-density-wave compounds.

A. The metal-insulator transition

In the presence of an increasing magnetic field, the electrons are confined to successively lower Landau levels. This is reflected experimentally by Shubnikov–de Haas oscillations, shown for sample S2 oriented along H in Fig. 1. The extreme quantum limit, where all the electrons populate the lowest spin-polarized Landau level, has been reached by $H \sim 1.5 \text{ kOe}$. Once the system is in the extreme quantum limit, the Fermi wave vector $k_F = 2\pi^2 n l^2$ is set by the magnetic length l , and the Fermi temperature drops with H as $T_F = \hbar^2 k_F^2 / 2m^* k_B = 12/H^2(\text{K})$ (S1) [$37/H^2$ (K) (S2)] for H in kOe. The potential-energy scale for electrons interacting with charged impurities is set by an effective Rydberg $k_B T^* = \hbar^2 / 2m^* a_B^{*2}$; here we have $T^* \sim 4 \text{ K}$ (S1) [11 K (S2)] and $a_B^* \sim 1000 \text{ \AA}$ (S1) [850 \AA (S2)]. Given that

$n^{1/3}a_B^* \approx 0.5$, the Coulomb interaction between electrons is on a comparable energy scale to $k_B T^*$.

As the magnetic field is increased into the extreme quantum limit, the size of an electron wave packet shrinks in the direction transverse to the field. We observe a sharp rise in ρ_{zz} , ρ_{xx} , and ρ_{xy} at critical magnetic field, $H_c(T)$, which marks the transition from metal to insulator. We reported³² earlier the apparent three-dimensional nature of this transition as indicated by the identical behavior (within a prefactor) near H_c of the conductivity parallel to and perpendicular to H . We follow the resistance along the magnetic field direction, R_{zz} , to higher H and T in Fig. 2. At any temperature, there are three regimes. At low magnetic field, the sample is metallic and the resistance is small. At a critical field, H_c , which is dependent on T , there is a sharp rise in the resistance associated with the onset of the insulating state. Finally, there is a third regime (seen most clearly at low T) where the rate of increase of the resistance slows for intermediate H , only to quicken again at highest field. We do not have a model for this complicated transport behavior, but the rapid rise of R_{zz} at high H argues against the presence of surface layer conduction which would act to saturate the resistance.^{32,33}

We also present the Hall resistivity, ρ_{xy} , as a function of H and T for S2 in Fig. 3. The data were taken using a van der Pauw technique to avoid mixing in components of ρ_{xx} which is comparable in magnitude. At low field there is a gradual temperature-independent rise in ρ_{xy} , consistent with the simple metallic relation $d\rho_{xy}/dH = 1/nec$. There is once again a sharp rise in ρ_{xy} at $H_c(T)$, which continues smoothly to the highest field measured, $H = 75$ kOe. The critical field determined from these ρ_{xy} curves is the same within 10% as that derived from ρ_{xx} or ρ_{zz} data. We determine H_c by the

linear extrapolation of the ρ_{xy} curves to the temperature-independent baseline, and we plot H_c as a function of T in Fig. 4. The solid line is a least-squares fit: $H_c = 9.8 + 4.4 T$ for T in K and H_c in kOe.

The linear dependence of H_c on T differs from the BCS-like dependence

$$T_c = 1.14 T_F \exp[-(\pi/\phi_0)(T_F/T^*)^{1/2}]$$

(here ϕ_0 is a number of order unity, weakly dependent on H) suggested by Fukuyama³⁴ for the phase boundary of a continuous charge-density-wave transition, and in good agreement with experiments on graphite at very high fields.¹⁰ However, these calculations were performed in the weak-coupling limit $T^*/T_F \ll 1$, which is not appropriate here. In the strong-coupling limit, a much weaker than exponential dependence is expected³⁴ and Gerhardt⁶ finds $T_c = (4\phi_0/\pi)(T_F/T^*)^{1/2}$, giving T_c decreasing as $1/H_c$ at high fields, which is also inconsistent with our data. The assumption of a continuous charge-density-wave transition is suspect in this system,^{6,35} given that $T_F/T_c \sim 1$. A better starting point is to consider the melting transition of a Wigner crystal, which is likely to be first order.

The theory of Kleppman and Elliott⁵ yields a value $H_c \sim 4-5$ kOe (S2) [3-4 kOe (S1)] as the critical field needed to induce a Wigner transition. This is close to the value that one would obtain from taking $n^{1/3}l = 0.2$ for a Mott insulator, and is within a factor of 2 of our data at $T=0$. Although no calculations for finite temperatures exist, if we estimate the melting temperatures to be $\frac{1}{8}$ the cohesive energy per electron, we obtain $dT_c/dH = 0.25$ K/kOe (0.3 K/kOe) for $H_c(T=0) = 9.8$ kOe (6.5 kOe), close to the experimental value of 0.3 K/kOe (0.22 K/kOe).

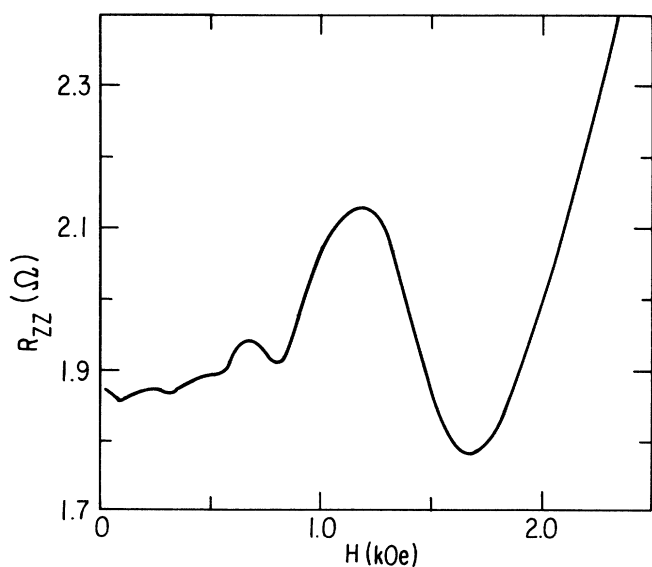


FIG. 1. The resistance R_{zz} parallel to the magnetic field H direction, showing Shubnikov-de Haas oscillations in sample S2 at $T = 10$ mK. The extreme quantum limit has been reached by $H \sim 1.5$ kOe.

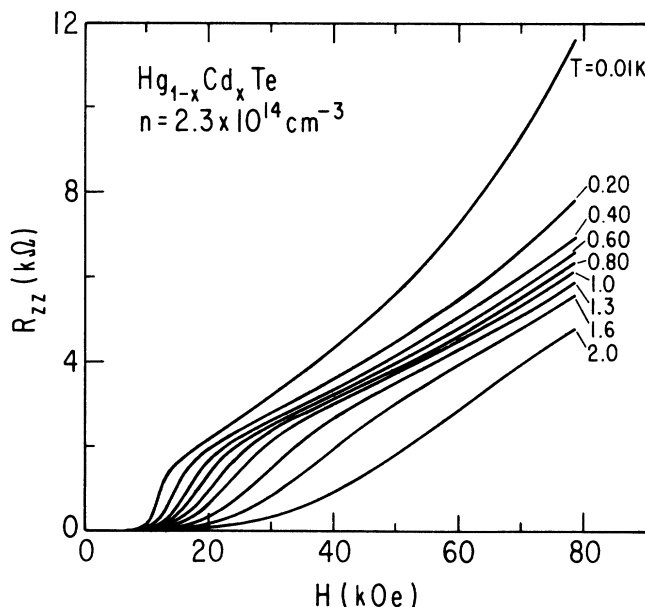


FIG. 2. The metal-insulator transition driven by magnetic field H for S2 at various temperatures T .

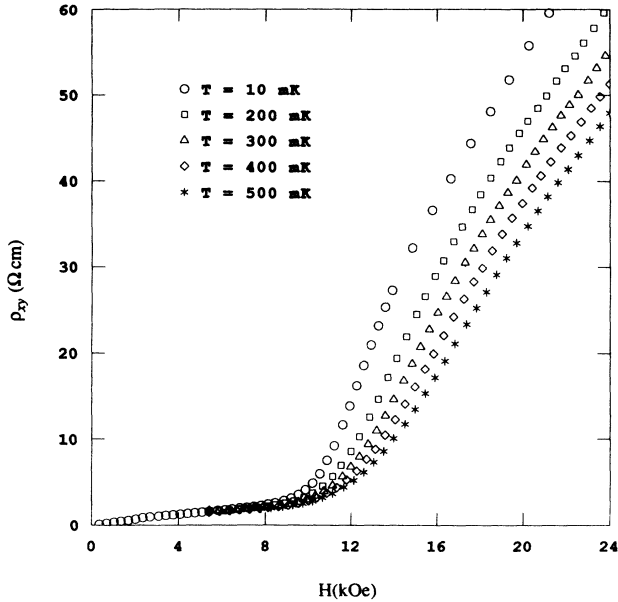


FIG. 3. The Hall resistivity ρ_{xy} through the metal-insulator transition for S2 at different temperatures.

Within the context of an electron lattice in magnetic field, we expect that a sample with low electron density will crystallize at a lower magnetic field than a sample with high n . The H_c -versus- T data from Hall-resistivity measurements³² on S1 ($n = 1.4 \times 10^{14} \text{ cm}^{-3}$) fits a linear relation $H_c = 6.5 + 4.5 T$ for T in K and H_c in kOe. Comparing this to the fit for S2 ($n = 2.3 \times 10^{14} \text{ cm}^{-3}$), we

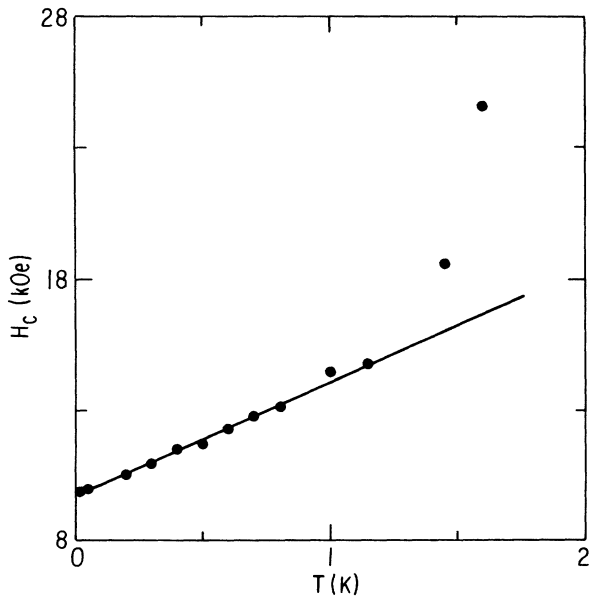


FIG. 4. The critical magnetic field H_c for the metal-insulator transition as a function of T , deduced from the linear extrapolation of ρ_{xy} to a temperature-independent background. The solid line is a least-squares fit to $H_c = 9.8 \text{ kOe} + 4.4 T$ (T in K), a form which naturally follows from the idea of a melting transition between electron crystal and correlated fluid.

find $[H_c(S1)]/[H_c(S2)] = 0.67$. This compares favorably to the ratio 0.61 obtained from the theory of Kleppman and Elliott.^{5,35}

At high magnetic field, the cohesive energy of a Wigner lattice should tend towards a constant¹ given by $1.79 k_B T^* / r_s$, where $4\pi r_s^3 = 1/n a_B^3$. In sample S2, this would lead to a saturation of T_c at about 2 K in high H . We see the beginning of such a saturation in the highest-temperature points of Fig. 4. This is a regime where thermal fluctuations dominate any quantum-mechanical effects. We plot in Fig. 5 T_c as a function of H to almost 100 kOe. The critical fields, H_c , were determined here from the points of maximal slope in Fig. 2, a technique which is more reliable at high T than extrapolation, but which overestimates the true values at all T .

Figure 5 represents a phase diagram for the $\text{Hg}_{1-x}\text{Cd}_x\text{Te}$ system in magnetic field at finite temperature. The data points lie on the phase boundary between a high- T -low- H correlated electron fluid, and a low- T -high- H electron solid. It emphasizes the importance of millikelvin temperatures for studying the properties of the electron solid.

Nimtz *et al.*³⁶ have argued that the linear relation $H_c \propto T$ found at millikelvin temperatures is the low- T extension of their measurements of a critical magnetic field for the onset of activated magnetotransport in the electron liquid. We maintain that these are very different physical processes,³⁷ and we plot in Fig. 6 their data from Ref. 36 on our phase diagram, Fig. 5. We see explicitly that the critical behavior of the electron solid does not continue linearly to $T = 10$ K, but saturates at $T \sim 2$ K, as discussed above. Nimtz *et al.* are measuring the properties of the correlated fluid at kelvin temperatures, as distinct from the behavior of the electron solid at millikel-

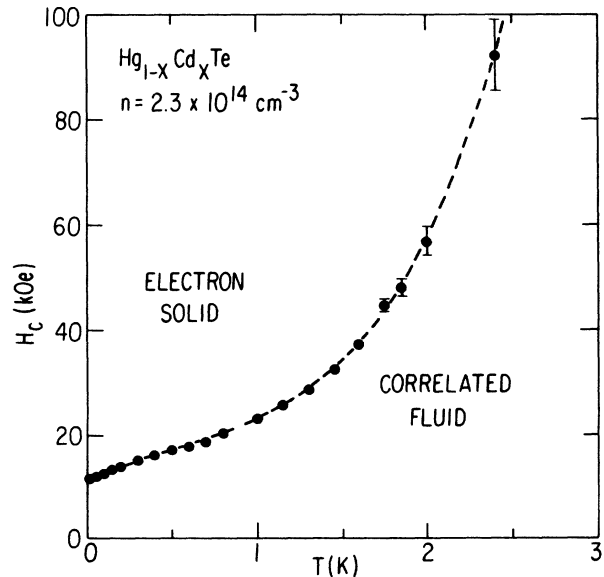


FIG. 5. The H - T phase diagram for S2 as determined by the points of maximal slope in R_{zz} vs H (Fig. 2). The dashed line is a guide to the eye, separating a high- T -low- H electron liquid from a low- T -high- H electron solid. Millikelvin temperatures are essential for studying correlation and disorder in the solid.

vin. Finally, we reiterate that the linear relation, $H_c \propto T$, follows naturally from the idea of a melting transition between Wigner crystal and correlated fluid.

B. Nonlinear I - V characteristics

The nature of the insulating state can only be inferred from the Ohmic magnetotransport measurements discussed above. We turn to the charge-density-wave analogy for a more direct probe of the relative roles of electron order and impurity disorder at high H and low T . We plot in Fig. 7 the non-Ohmic response of $S2$ for $E < 1$ mV/cm. At $T=10$ mK and $H=27$ kOe, the sample is firmly in the electron solid portion of the phase diagram (Fig. 5).

The data in the top half of the figure were obtained through a direct measurement of the differential resistance, while the Ohmic portion, V/R_0 , has been subtracted from the curve in the bottom half. In both cases, deviations from zero represent non-Ohmic character and an increase in the conductivity. The electric field for the onset of the nonlinear conduction process is well defined by the dc method, but observable by either method.

We posit that the sharp threshold at such a small electric field is analogous to the depinning field observed³⁸ in charge-density-wave compounds and associate the nonlinear conductivity with the sliding of electron crystal domains. We have previously³⁹ ruled out heating as the cause for the behavior observed in Fig. 7 and, in fact, we observe a second region (at the same H and T) of non-Ohmic behavior which is simple I^2R heating at $\sim 10^4$ times the power level here.

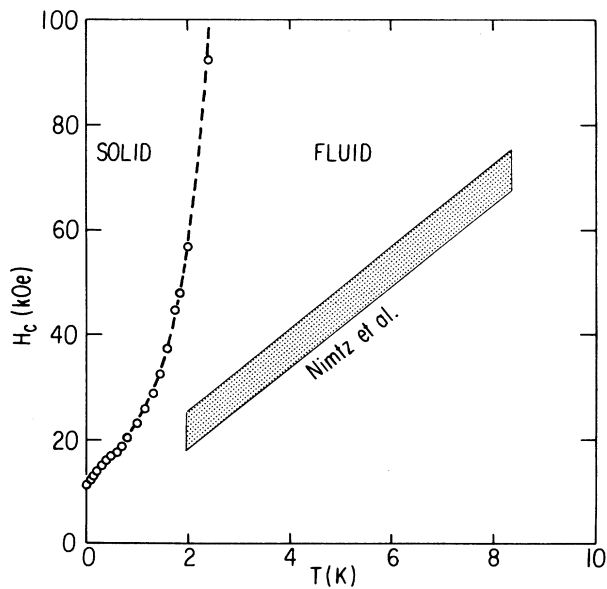


FIG. 6. The phase diagram of Fig. 5 expanded to show the region (shaded, Ref. 36) in which Nimtz *et al.* have defined a critical magnetic field by the onset of activated magnetotransport. Their measurements probe the properties of the correlated fluid; our H_c defines the transition from electron solid to fluid and saturates at $T \sim 2$ K.

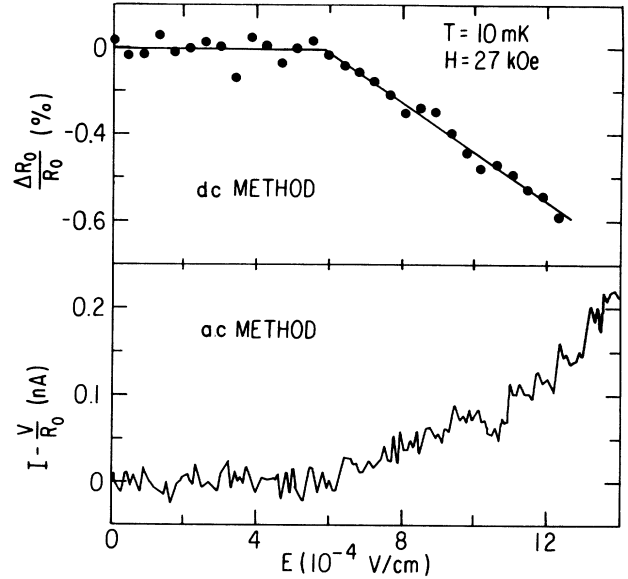


FIG. 7. The onset of nonlinear conduction in the insulator at a threshold electric field $E_d < 1$ mV/cm. The dc and ac methods are described in the text. The tiny E_d indicates a collective effect; we estimate a correlation length for the electron crystal by analogy to theory⁹ for charge-density-wave compounds.

We believe that impact ionization of the electrons is an untenable explanation as well. At $T \sim 1$ K and $H=0$, impact ionization has been observed⁴⁰ in similar stoichiometry $\text{Hg}_{1-x}\text{Cd}_x\text{Te}$ at threshold electric fields of 15 V/cm. Here we measure a depinning field, E_d , 5 orders of magnitude smaller and we have found³⁹ only a very weak temperature dependence to E_d for $10 < T < 200$ mK. Finally, we note that the nonlinear

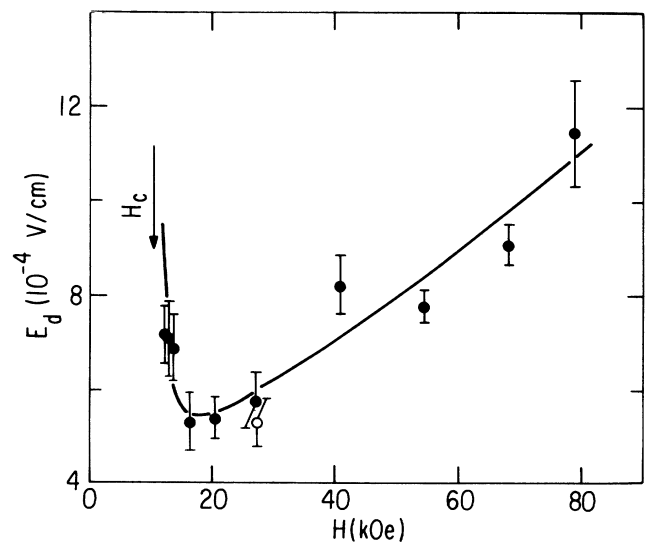


FIG. 8. Magnetic field H dependence of the threshold electric field for depinning, E_d , for $S2$ at $T=10$ mK. Solid circles (open circle) were determined via the ac (dc) method. The solid line is a guide to the eye, but follows an $H^{4/3}$ dependence for $H > 20$ kOe (see text).

conduction region in both $S1$ and $S2$ is accompanied by a large increase in the noise, similar to results³⁸ on sliding charge-density-wave compounds.

The very low electric fields for the onset of nonlinear conductivity [$E_d = 6 \times 10^{-4}$ V/cm ($S2$); 3×10^{-4} V/cm ($S1$)] cannot be accounted for by the field ionization of single electrons from impurities. If we apply the scaling approach⁹ for the depinning of a charge-density wave outlined in the theory section above, then we find $L/R_0 \sim 150$ ($S2$) [~ 200 ($S1$)] at $H = 27$ kOe and $T = 10$ mK. The electrons remain correlated over a few hundred lattice spacings, $n^{-1/3}$, which gives a correlation length of tens of micrometers. We find $[E_d(S1)]/[E_d(S2)] \sim 0.5$ at low T and for any $H > H_c$. The larger depinning field (smaller correlation length) in $S2$ is presumably a function of the greater disorder introduced by a higher donor density. We also find that the change in conductivity upon depinning is a factor of 3 lower in $S2$ than in $S1$. The correlated electron domains may find it more difficult to slide over a larger concentration of ionized impurities, but any quantitative treatment of the ratio of the nonlinear to the linear conductivity must involve a detailed understanding of the relaxation mechanisms of the different conduction processes present.

We can go beyond the mere analogy to charge-density-wave systems because of the extra experimental parameter in the $\text{Hg}_{1-x}\text{Cd}_x\text{Te}$ case: magnetic field. We plot in Fig. 8 the variation in E_d with H at $T = 10$ mK for $S2$. The arrow marking H_c was determined independently from the Hall resistivity (Fig. 3).

Figure 8 allows us insight into the different regimes of the electron (poly)crystal. At $H \sim H_c$ the elastic modulus K presumably is reduced by fluctuations, and since $E_d \propto K^{-3}$, the depinning field rises as H_c is approached from above. The domains are "squishy" and a larger electric field is required to make them slide in concert. As H is increased, the crystal becomes stiffer, the correlation length increases, and E_d decreases. At sufficiently high H , however, the electron-impurity interaction will dominate as the electron wave function shrinks and it is affected more strongly by the random potential. The correlated regions become smaller and E_d increases again; for $H \rightarrow \infty$ the system must reach magnetic freeze-out. If Φ scales with magnetic length as $l^{-2/3}$, as is the case for an electron bound in a Coulomb well, then $E_d \propto l^{-8/3} \propto H^{4/3}$. The solid line in Fig. 8 follows an $H^{4/3}$ law for $H > 20$ kOe.

V. CONCLUSIONS

To good measure, the debate about the meaning of magnetotransport measurements on narrow-gap semiconductors has been polarized between advocates of Wigner crystallization and proponents of magnetic freeze-out. Yet, the energy scales for electron-electron and electron-impurity interactions are similar. We believe that both correlation and disorder must be considered in analyzing the data, and we discover a nonlinear conduction process in the magnetic-field-driven insulating state which allows us to quantitatively account for the relative role of in-

teractions and randomness through the determination of a correlation length for the electron lattice. We explicitly map out the H - T phase diagram for the melting of the electron (poly)crystal and find a linear relation between critical field and temperature which follows from the theory for a Wigner crystal in magnetic field. The critical field saturates at a few kelvin, demonstrating that millikelvin temperatures are essential for studying the properties of the electron solid.

A brief summary of our picture is as follows. At any temperature less than the Landau-level splitting, there will be a crossover from delocalized electronic states to a highly correlated electron fluid at a typical magnetic field such that $n^{1/3}l \sim 0.2$. At sufficiently low temperature, e.g., $T \sim 0.2T^*/r_s$ reached in our dilution refrigerator, the electrons solidify. The system balances the effects of electron ordering and disorder by forming domains. Although the large size of the electron wave packets helps average over the random potential, even weak disorder is sufficient to pin the correlated regions of electrons to the underlying crystal by introducing fluctuations on a length scale $\gg n^{-1/3}$. In analogy to depinning experiments on charge-density-wave compounds, we find nonlinear I - V characteristics for $E < 1$ mV/cm which imply a correlation length $L \sim 200n^{-1/3}$. The electrons appear to order on a length scale of tens of micrometers. At the same time, the disorder permits donor-bound electrons, with likely concentrations on domain walls. Vacancies propagating along these domain boundaries²⁶ may also contribute to the unusual transport properties at high H and low T .

Recent measurements of cyclotron resonance^{41,42} in similar samples to ours have shown sharp transitions which have been interpreted in terms of hydrogenically bound impurity states with a concentration comparable to the total carrier concentration n . Sharp resonances would also be expected even in a perfect crystalline arrangement of electrons because the carriers are localized, although the dependence of the transition energy on magnetic field will be different from the $H^{1/3}$ dependence in the case of a hydrogenic donor. The field dependence in the case of the Wigner crystal has not been calculated to our knowledge, and depends in detail on the form of the wave function. Yet, a gradual increase in the transition energy with field as the electrons become more tightly bound is to be expected. Given that the localizing potential certainly does not diverge as $1/r$, we suspect that the behavior might easily mimic that of a hydrogenic donor with a large central-cell correction, the form used by Choi *et al.*⁴² to fit their data. Furthermore, to complicate the interpretation, the disorder which is present in a system with a finite correlation length provides additional sites for actual electron-impurity orbits.

ACKNOWLEDGMENTS

The work at The University of Chicago was supported by the National Science Foundation under Grant No. DMR85-17478. One of us (T.F.R.) acknowledges support from the Alfred P. Sloan Foundation.

- *Present address: Physics Department, Massachusetts Institute of Technology, Cambridge, MA 02139.
- ¹E. Wigner, *Phys. Rev.* **46**, 1002 (1934).
 - ²See J. M. Ziman, *Principles of the Theory of Solids*, 2nd ed. (Cambridge University Press, Cambridge, 1972), p. 65.
 - ³See N. F. Mott, *Metal-Insulator Transitions* (Taylor and Francis, London, 1974).
 - ⁴J. Durkan, R. J. Elliott, and N. H. March, *Rev. Mod. Phys.* **40**, 812 (1968).
 - ⁵W. G. Kleppman and R. J. Elliott, *J. Phys. C* **8**, 2729 (1975).
 - ⁶R. R. Gerhardts, *Solid State Commun.* **36**, 397 (1980).
 - ⁷A. L. Efros and B. I. Shklovskii, *J. Phys. C* **8**, L49 (1975).
 - ⁸C. M. Care and N. H. March, *J. Phys. C* **4**, L372 (1971).
 - ⁹H. Fukuyama and P. A. Lee, *Phys. Rev. B* **17**, 535 (1978); P. A. Lee and T. M. Rice, *ibid.* **19**, 3970 (1979); H. Fukuyama and P. A. Lee, *ibid.* **18**, 6245 (1978).
 - ¹⁰Y. Iye, P. M. Tedrow, G. Timp, M. Shayegan, M. S. Dresselhaus, A. Furukawa, and S. Tanuma, *Phys. Rev. B* **25**, 5478 (1982); G. Timp, P. D. Dresselhaus, T. C. Chieu, G. Dresselhaus, and Y. Iye, *ibid.* **28**, 7393 (1983).
 - ¹¹H. Celli and N. D. Mermin, *Phys. Rev.* **140**, A839 (1965); B. I. Halperin, in *Condensed Matter Theories*, edited by P. Vashista *et al.* (Plenum, New York, 1987), Vol. 2.
 - ¹²See, for example, P. Pieranski, *Contemp. Phys.* **24**, 25 (1983); H. M. Lindsay and P. M. Chaikin, *J. Chem. Phys.* **76**, 3774 (1982).
 - ¹³J. P. Schiffer and P. Kierle, *Z. Phys. A* **321**, 181 (1985); E. N. Dementiev, N. S. Dikansky, A. S. Medvedko, V. V. Parkhomchuk, and D. V. Pestrikov, *Zh. Tekh. Fiz.* **50**, 1717 (1980) [*Sov. Phys.* — *Tech. Phys.* **25**, 1001 (1980)].
 - ¹⁴C. C. Grimes and G. Adams, *Phys. Rev. Lett.* **42**, 795 (1977).
 - ¹⁵For details on the properties of the $\text{Hg}_{1-x}\text{Cd}_x\text{Te}$ system, see R. Dornhaus and G. Nimtz, in *Narrow Gap Semiconductors*, Vol. 98 of *Springer Tracts in Modern Physics*, edited by G. Höhler and E. A. Niekisch (Springer-Verlag, Berlin, 1983).
 - ¹⁶D. A. Nelson, W. M. Higgins, R. A. Lancaster, R. P. Muro-sako, and R. G. Roy (unpublished).
 - ¹⁷J. B. Mullin and A. Royle, *J. Phys. D* **17**, L69 (1984).
 - ¹⁸W. Zhao, C. Mazure, F. Koch, J. Ziegler, and H. Maier, *Surf. Sci.* **142**, 400 (1984).
 - ¹⁹O. Caporaletti and W. Micklethwaite, *Phys. Lett.* **89A**, 151 (1982).
 - ²⁰L. Lou and W. Frye, *J. Appl. Phys.* **56**, 2253 (1984).
 - ²¹W. Scott, E. Stelzer, and R. Hager, *J. Appl. Phys.* **47**, 1408 (1976).
 - ²²C. C. Grimes and G. Adams, *Phys. Rev. Lett.* **42**, 138 (1977).
 - ²³L. J. van der Pauw, *Philips Res. Rep.* **13**, 1 (1958).
 - ²⁴A. P. Aleinikov, P. I. Baranskii, and A. V. Zhidkov, *Pis'ma Zh. Eksp. Teor. Fiz.* **35**, 464 (1982) [*JETP Lett.* **35**, 574 (1982)].
 - ²⁵B. Schlicht and G. Nimtz, in *Physics of Narrow Gap Semiconductors*, Vol. 152 of *Springer Lecture Notes in Physics*, edited by E. Gornik, H. Heinrich, and L. Palmetshofer (Springer-Verlag, Berlin, 1982), p. 383.
 - ²⁶C. M. Care and N. H. March, *J. Phys. C* **4**, L372 (1971); D. J. Somerford, *ibid.* **4**, 1570 (1971).
 - ²⁷J. Gebhardt, G. Nimtz, B. Schlicht, and J. P. Stadler, *Phys. Rev. B* **32**, 5449 (1985).
 - ²⁸A. Raymond, J. L. Robert, R. L. Aulombard, C. Bousquet, and O. Valassiades, in *Physics of Narrow Gap Semiconductors*, Ref. 25, p. 387.
 - ²⁹G. de Vos and F. Herlach, in *Applications of High Magnetic Fields in Semiconductors*, Vol. 177 of *Springer Lecture Notes in Physics*, edited by G. Landwehr (Springer-Verlag, Berlin, 1983), p. 378.
 - ³⁰J. L. Robert, in *Narrow Gap Semiconductors: Physics and Applications*, Vol. 133 of *Springer Lecture Notes in Physics*, edited by W. Zawadzki (Springer-Verlag, Berlin, 1980), p. 176.
 - ³¹M. Shayegan, V. J. Goldman, H. D. Drew, N. A. Fortune, and J. S. Brooks, *Solid State Commun.* **60**, 817 (1986); M. Shayegan, H. Drew, D. A. Nelson, and P. M. Tedrow, *Phys. Rev. B* **31**, 6123 (1985).
 - ³²T. F. Rosenbaum, S. B. Field, D. A. Nelson, and P. B. Littlewood, *Phys. Rev. Lett.* **54**, 241 (1985).
 - ³³J. P. Stadler, G. Nimtz, B. Schlicht, and G. Remenyi, *Solid State Commun.* **52**, 67 (1984).
 - ³⁴H. Fukuyama, *Solid State Commun.* **26**, 783 (1978); D. Yoshioka and H. Fukuyama, *J. Phys. Soc. Jpn.* **50**, 725 (1981).
 - ³⁵Y. Kuramoto, *J. Phys. Soc. Jpn.* **44**, 1572 (1978).
 - ³⁶G. Nimtz, J. Gebhardt, B. Schlicht, and J. P. Stadler, *Phys. Rev. Lett.* **55**, 443 (1985).
 - ³⁷T. F. Rosenbaum, S. B. Field, D. A. Nelson, and P. B. Littlewood, *Phys. Rev. Lett.* **55**, 444 (1985).
 - ³⁸For extensive reviews, see G. Gruner, *Physica* **8D**, 1 (1983); N. P. Ong, *Can. J. Phys.* **60**, 757 (1982).
 - ³⁹S. B. Field, D. H. Reich, B. S. Shivaram, T. F. Rosenbaum, D. A. Nelson, and P. B. Littlewood, *Phys. Rev. B* **33**, 5082 (1986).
 - ⁴⁰V. N. Kobaysev and A. S. Tager, *Pis'ma Zh. Eksp. Teor. Fiz.* **3**, 164 (1981) [*JETP Lett.* **14**, 107 (1971)]; G. Nimtz, G. Bauer, R. Dornhaus, and K. M. Muller, *Phys. Rev. B* **10**, 3302 (1974).
 - ⁴¹V. J. Goldman, H. D. Drew, M. Shayegan, and D. A. Nelson, *Phys. Rev. Lett.* **56**, 968 (1986).
 - ⁴²J. B. Choi, H. D. Drew, and D. A. Nelson, *Solid State Commun.* (to be published).